ISSN (Print) 1226-1750
ISSN (Online) 2233-6656
Journal of Magnetics 25(2), 245-253 (2020) https://doi.org/10.4283/JMAG.2020.25.2.245

A Facile Chemical Synthesis of Silica Coated FeCo Nanocubes

Komkrich Chokprasombat[1]* and Santi Maensiri[2]

[1]*Department of Physics, Faculty of Science, Thaksin University, Phatthalung 93210 Thailand*
[2]*School of Physics, Institute of Science, Suranaree University of Technology, Nakhon Ratchasima 30000 Thailand*

(Received 29 November 2019, Received in final form 16 June 2020, Accepted 17 June 2020)

FeCo nanostructures are of interest because of their high magnetization and low coercivity which are suitable for biomedical applications. However, particle morphologies are still difficult to control. In this work, the FeCo nanocubes have been prepared by a chemical reduction method using hydrazine as a reducing agent. Using only polyvinylpyrrolidone (PVP) as a capping agent without cyclohexane as previous works, the obtained particles are quite uniform in shape and air-stable, and can be facile coated with silica. Nevertheless, to obtain the uniform FeCo nanocubes, the concentration of sodium hydroxide used in the synthesis needs to be optimized. The obtained FeCo nanocubes exhibit a high saturation magnetization of 220.9 emu/g and low coercivities of around 180 Oe.

Keywords : nanostructures, FeCo, chemical reduction, silica coating

1. Introduction

Shape-controlled synthesis of nanoparticles is one of the major challenges in nanotechnology [1]. Many physical properties of synthesized nanoparticles are found to depend on their shape [2-4]. For example, with the same particle volume, coercivity of cobalt ferrite nanocubes is remarkably lower than that of the spherical particles, owing to the smaller surface anisotropy in the cubic nanocrystals [4]. Particles with a cubic shape are also important in biosensing applications due to larger contact area compared to the spherical shape [5]. In addition, self-assembly of magnetic nanocubes offers a simple route to fabrication of magnetic nanodot arrays for using in the ultrahigh magnetic recording [6]. Recently, a number of metal, oxide and alloy nanocubes have been synthesized including Ag, $CoFe_2O_4$, Fe_3O_4, FePt, PtCo [1, 4, 6-8]. However, there are a few works that demonstrate a successful preparation of FeCo nanocubes.

FeCo alloy has gained much attention in recent years due to its excellent magnetic properties such as low coercivity (H_c), high permeability, and high saturation magnetization (M_s) [9-11]. These magnetic properties can increase efficiency in theranostic applications such as MRI contrast enhancement and magnetic hyperthermia cancer treatment [12, 13]. Furthermore, the detectability of magnetic biosensors can be increased by using magnetic particles with higher M_s and larger diameter [14]. Besides, thanks to the very high M_s of FeCo nanoparticles, the decrease of M_s due to coating with organic or inorganic materials may not be concerned. Regarding several advantages of FeCo alloy, a lot of works have been devoted to the synthesis and characterization of the FeCo nanoparticles [15-20].

In an initial work, Kodama *et al.* prepared sub-micrometer-sized FeCo dices by a modified polyol process. They found that shape of the FeCo particles strongly depends on the amount of particle compositions [21]. Subsequently, Wei and colleagues successfully synthesized FeCo nanocubes by a chemical reduction method in which metal ions were reduced by hydrazine monohydrate in the presence of cyclohexane and polyethylene glycol (PEG-400) [22]. They found that the amount of cyclohexane and PEG-400 need to be optimized to obtain the particles with a well-defined cubic shape. Recently, we synthesized FeCo nanocubes by such chemical reduction process in which PEG-400 was replaced with varied amounts of PEG-8000. We found that the excessive PEG-8000 promotes the presence of large polyhedral-shape particles, and the saturation magnetization, remanent magnetization, and coercivity of the polyhedral-shape particles are lower than those of the cubic particles due to

©The Korean Magnetics Society. All rights reserved.
*Corresponding author: Tel: +66-0-7460-9600
Fax: +66-0-7460-9600, e-mail: komkrich@tsu.ac.th

© 2020 Journal of Magnetics

the difference in shape anisotropy [23]. FeCo nanocubes prepared by this reduction method were also coated with silica (SiO_2) and further functionalized with amine for using in biosensors [24]. However, the direct deposition of silica on pure metal particles is quite difficult [25]; therefore, as in [24], the as-prepared particles have to be coated with polyvinylpyrrolidone (PVP) before further coating with the silica.

In this work, we propose a facile synthesis of FeCo nanocubes by the chemical reduction process using only PVP as the capping polymer. The particles with a well-defined cubic shape could be obtained even though cyclohexane was not used. Moreover, to demonstrate a benefit of our synthesis, silica, a well-known material for nanoparticle coating, was directly coated on the particle surfaces without any surface modifications. The silica-coated FeCo nanocubes could be further functionalized for advanced applications.

2. Experimental

2.1. Synthesis of FeCo nanocubes

All chemicals were bought from Sigma Aldrich Co. and used as received. In ambient environment, 2 g of PVP (m_W ~ 55000 g/mol), 0.695 g (2.5 mmol) of $FeSO_4 \cdot 7H_2O$, and 0.595 g (2.5 mmol) of $CoCl_2 \cdot 6H_2O$ were dissolved in 50 mL of deionized water (DI-water) within an Erlenmeyer flask. After dissolving the starting materials, a glass pipette connected with an Ar gas line was immersed in the solution, and Ar gas was flowed for 20 min to remove dissolved oxygen (Ar purging). Next, the flask was quickly sealed with aluminium foil and then sonicated for 90 min. The sonicated solution was then heated to 80 °C in an oil bath. Subsequently, a prepared solution of 2.5 g of sodium hydroxide (NaOH) dissolved in 20 mL of hydrazine monohydrate (NH_2-$NH_2 \cdot H_2O$, 85 wt%) was slowly injected into the solution by a syringe (~10 mL/min). The reaction was dwelled at 80 °C for 30 min before cooled down to room temperature naturally. The black precipitate was separated using a permanent magnet and subsequently washed with DI-water for 5 times and acetone for 3 times. The obtained powder was air-stable and could be dried in an oven at 60 °C for 2 hours [26]. To investigate effects of PVP and NaOH concentrations, the mentioned synthetic procedure was repeated multiple times with different amounts of PVP or NaOH. Five samples were referred to S1, S2, S3, S4, and S5 according to the different amounts of PVP and NaOH used in each sample (detailed in Table 1).

2.2. Silica coated FeCo nanocubes

The process of silica coating was adapted from the previous report [24]. In brief, 20 mg of as-prepared FeCo nanocubes (sample S2) was dispersed in 20 mL of ethanol with the presence of 2.2 mL of DI-water. The mixture was sonicated for 60 min, and then stirred mechanically. Subsequently, 1.5 mL of 25 % ammonium hydroxide (NH_4OH) and 0.1 mL of tetraethylorthosilicate (TEOS) were in order added to the mixture, which was further mechanically stirred for 6 hours. The silica coated FeCo nanocubes were separated using a permanent magnet and washed several times with ethanol and DI-water.

2.3. Nanoparticle characterizations

Crystal structures of the as-prepared particles were determined by X-ray powder diffractometer (XRD, Bruker D2 phaser), which was operated with Cu-Kα radiation (λ = 1.54060 Å), and the 2θ angle was varied from 20 to 100 degree. Transmission electron microscope (TEM, FEI Tecnai G^2 20) was performed at 200 keV to examine size and shape distributions of the particles as well as a core-shell structure of silica coated particles. Field-emission scanning electron microscope (FE-SEM, JEOL JSM-7800F) was also used to verify the particle shape. The elemental compositions were analyzed by energy-dispersive X-ray spectroscopy (EDS, Oxford Instruments) equipped with the TEM, which was performed for 4 times in different particle areas to get an average value. The magnetic moments of the particles were measured by a vibrating sample magnetometer (VSM, VersaLab Quantum Design) at 300 K. The applied magnetic field was varied between –30 and 30 kOe.

Table 1. Synthetic conditions and elemental compositions of as-prepared FeCo particles.

Sample	Amount of reactants used				Elemental composition (at %)	
	$FeSO_4 \cdot 7H_2O$ (g)	$CoCl_2 \cdot 6H_2O$ (g)	PVP (g)	NaOH (g)	Fe	Co
S1	0.695	0.595	0	2.5	45.68	54.32
S2	0.695	0.595	2	2.5	55.35	44.64
S3	0.695	0.595	4	2.5	54.58	45.42
S4	0.695	0.595	2	1.5	54.74	45.25
S5	0.695	0.595	2	3.5	52.27	47.82

3. Results and Discussion

In the previous report [22], shape of the particles strongly depends on the concentration of PEG-400 and cyclohexane. The optimized concentration needs to be used to obtain the particles with a well-defined cubic shape. By using the non-optimized concentrations, a lot of irregular FeCo nanoplates with some nanorods and nanocubes are obtained. In the present work, we replace PEG-400 with PVP, and synthesize FeCo nanocubes without cyclohexane. The amounts of PVP and NaOH are varied (Table 1) to examine their effects on crystallinity, morphology, composition and magnetic properties of the particles.

3.1. XRD characterization

Figure 1 illustrates the XRD spectra of the as-prepared particles. All samples are well-crystalline and clearly matching with the standard cubic FeCo alloy (JCPDS No. 44-1433). The apparent peaks can be identified as the (110), (200), and (211) reflections. No metal oxides or additional peaks found in the spectra indicate that all samples are single-phase and air-stable. Figure 1(a) compares the XRD patterns of the samples S1, S2, and S3 in which 2.5 g (1.25 M) of NaOH was used, and the amount of PVP was varied as 0, 2, and 4 g, respectively. It is evidently seen that the concentration of PVP does not affect the crystalline structure of the as-prepared FeCo particles. Although the PVP is not used, the FeCo particles with well-crystalline structure could also be obtained. These consequences imply that the dissolved metal ions are easily reduced by hydrazine monohydrate under a concentrated basic condition and rapidly formed to the FeCo alloy. Regarding a previous report [27] in which at least 0.75 M of NaOH need to be used to eliminate the secondary phase such as $CoFe_2O_4$; The NaOH concentration was thus altered as 0.75, 1.25, and 1.75 M in the preparation of samples S4, S2, and S5, respectively. These concentrations are enough to obtaining the single-phase FeCo. The average lattice parameters of the samples S1, S2, S3, S4, and S5 determined from the positions of the apparent peaks in each XRD spectrum are 2.8563, 2.8533, 2.8495, 2.8521, and 2.8482, respectively. These values are slightly less than the standard value 2.8570 of bulk FeCo alloy which may originate from the small size and disordered orientation of the particles [28].

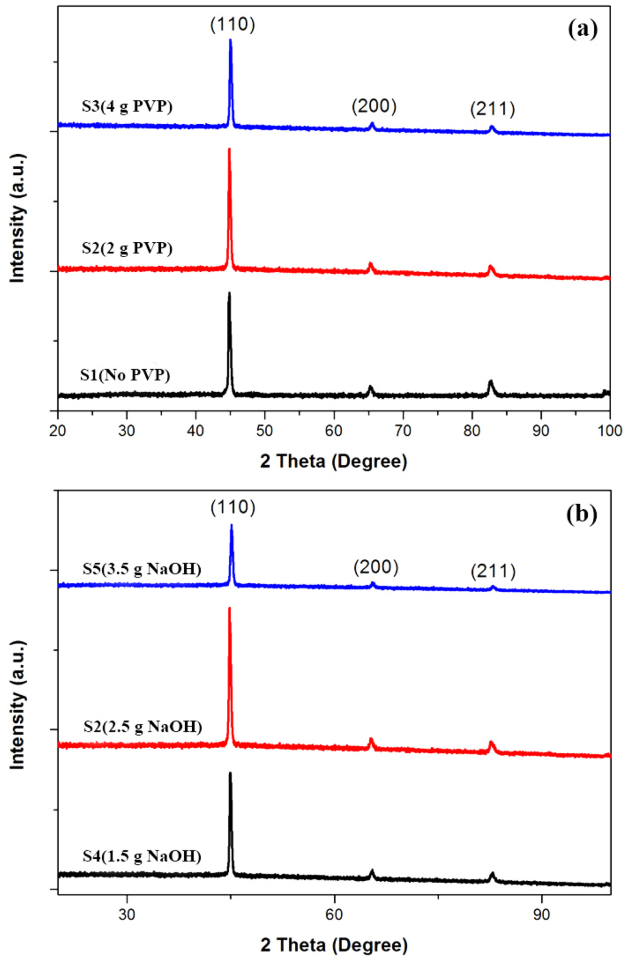

Fig. 1. (Color online) XRD Patterns of the samples prepared with the same conditions except that (a) PVP was varied while NaOH was fixed at 2.5 g, and (b) NaOH was varied while PVP was fixed at 2.0 g.

3.2. SEM and TEM characterizations

The particle morphology was found to strongly depend on the concentrations of PVP and NaOH. To obtain the well-defined shape FeCo nanocubes, 2.0 g of PVP and 2.5 g of NaOH need to be used in the sample preparation. Figure 2 shows the SEM and TEM characterizations of sample S2 in which the optimized concentrations of PVP and NaOH were employed. It is obviously seen that the as-prepared FeCo particles are cubic in shape and the isolated nanocubes can be obtained although the particles tend to agglomerate due to strong attractive forces [23]. A mean edge length of as-prepared FeCo nanocubes determined from a hundred of particles is 96 ± 17 nm which is moderately larger than 68 ± 6 nm that reported in the previous work [22]. The non-uniform in size of the particles might relate to the slow adding rate of the reducing agent, leading to the difference in particle growth time.

Selected area electron diffraction (SAED) pattern shown in Fig. 2(c) can be indexed to the diffraction planes of bcc FeCo alloy conforming to the XRD analysis. A SEAD pattern of an isolated particle (Fig. 2(d)) reveals a single-crystal characteristic which could be indexed to [001] zone of the cubic FeCo alloy. However, it should be noted

that some amorphous parts can be formed in the particles due to defect occurring during the growth process, and the presence of the coated polymer [23].

Figure 2(e) illustrates the EDS spectrum of the FeCo nanocubes deposited on a carbon-coated copper grid in which the characteristic peaks of Fe and Co are obviously indicated. The average atomic percentages of Fe and Co are approximately 55 and 45, respectively. The presence of negligible amount of oxygen in the spectrum may obtain from metal oxidations on the particle surfaces as

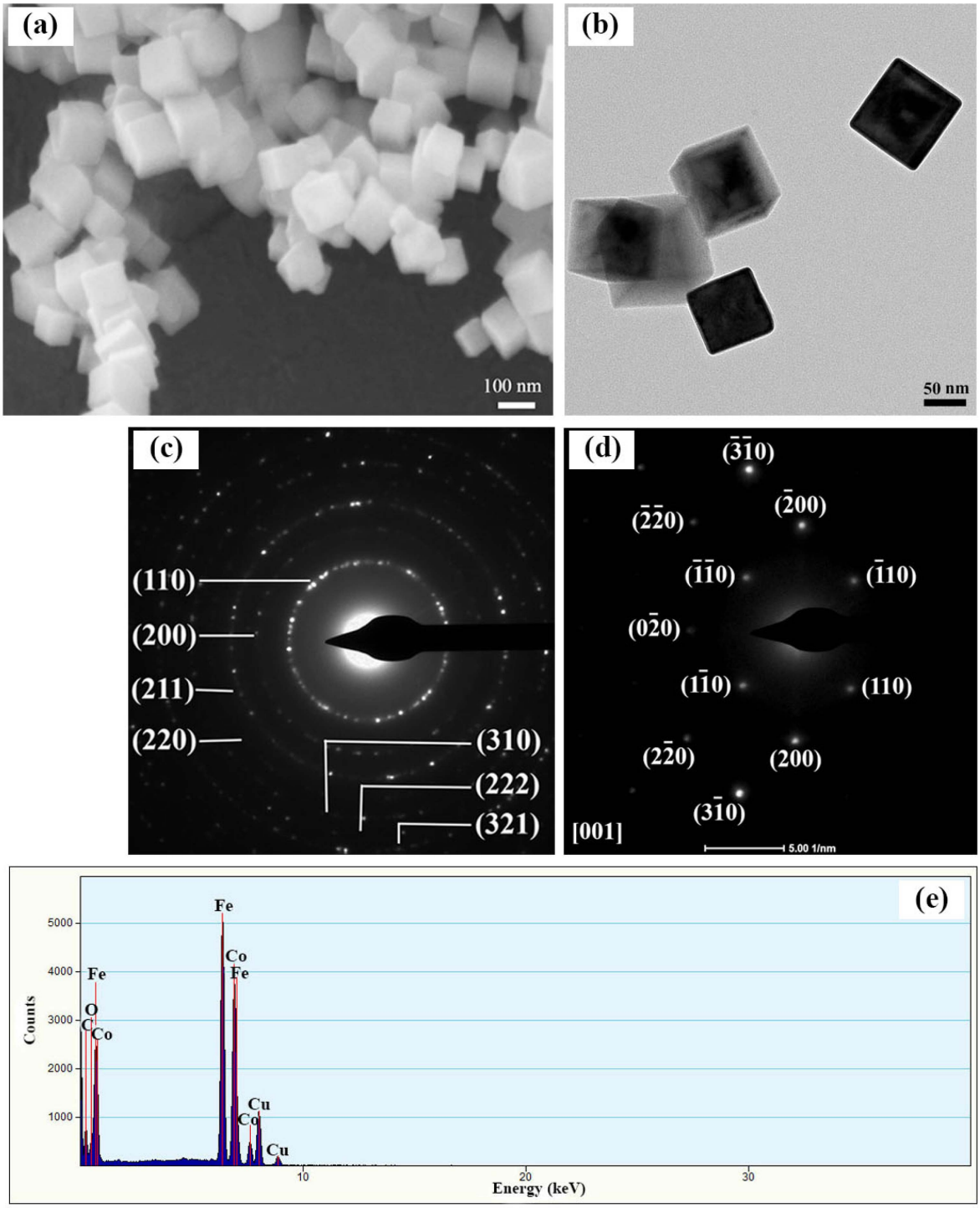

Fig. 2. (Color online) SEM and TEM characterizations of as-prepared FeCo nanocubes (sample S2). (a) SEM image, (b) TEM image, (c) SAED pattern diffracted from agglomerated FeCo nanocubes, (d) SAED pattern diffracted from an isolated FeCo nanocube, and (e) EDS spectrum of the FeCo nanocubes.

well as the presence of coating polymer. The EDS spectra of the other samples also have the similar profiles; however, as can be seen in Table 1, the Fe fraction of sample 1 is lower than that of the others which might relate to the absence of PVP. In the results of Wei *et al.* [22], the elemental composition of FeCo nanocubes could be

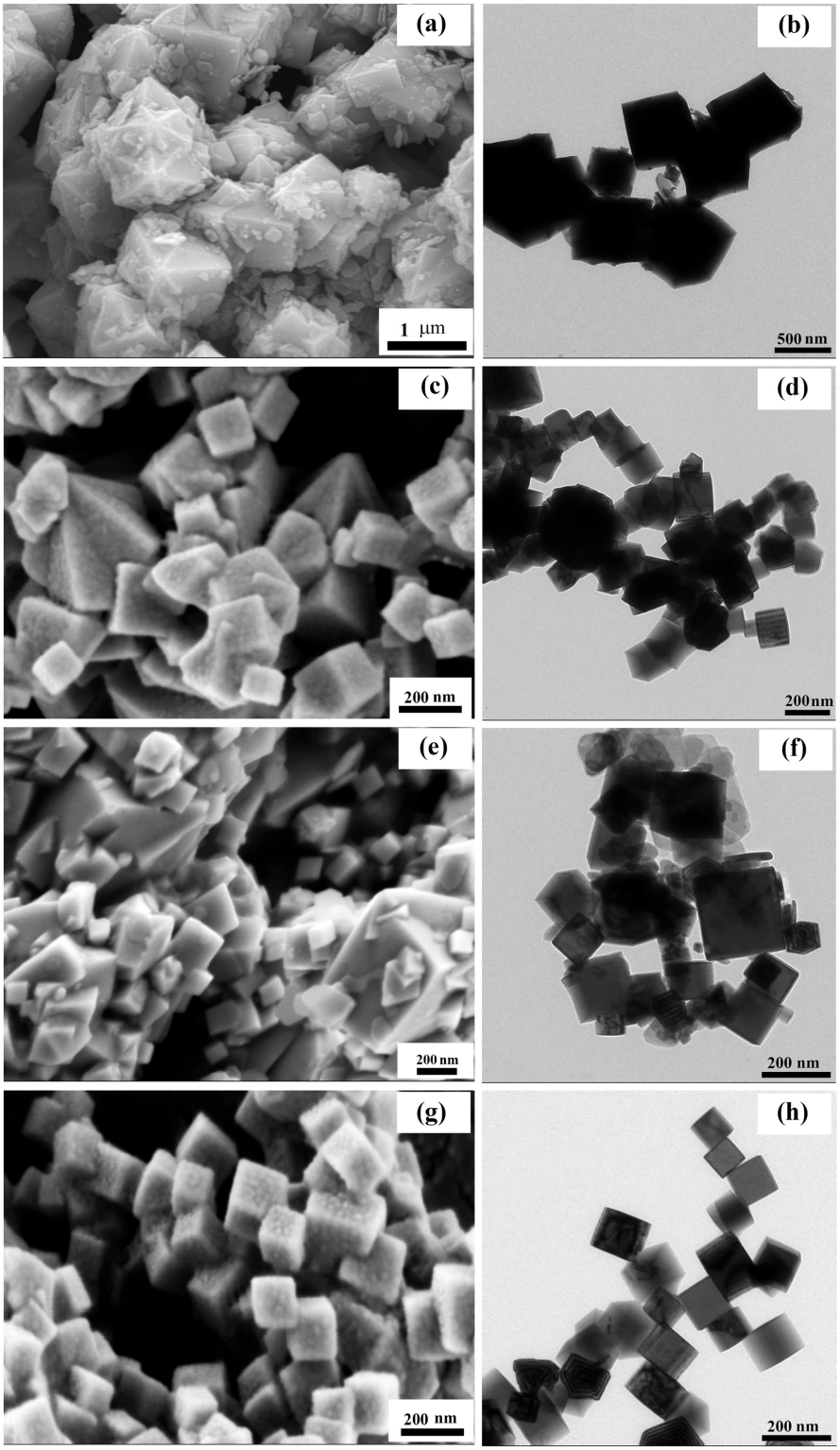

Fig. 3. SEM and TEM images of the samples. (a) SEM and (b) TEM images of sample S1, (c) SEM and (d) TEM images of sample S3, (e) SEM and (f) TEM images of sample S4, (g) SEM and (h) TEM images of sample S5.

approximated as $Fe_{50}Co_{50}$ indicating that all metal ions could be reduced and subsequently formed to FeCo alloy. In our work, the high molecular weight PVP was used instead which might affect to the reduction potentials of Fe^{2+}/Fe and Co^{2+}/Co redox pairs. The standard reduction potentials of Fe^{2+}/Fe and Co^{2+}/Co are −0.41 and −0.29 respectively [27]; therefore, Co^{2+} can be easier reduced to Co due to its more positive reduction potential. The easier reduction of Co^{2+} results the higher atomic percentage of Co found in sample S1. By contrast, when the PVP was used, the reduction potential of Fe^{2+}/Fe might be more positive leading to the higher atomic percentage of Fe. Additionally, as reported in [27], the excessive amount of NaOH could change the reduction potentials of Fe^{2+}/Fe and Co^{2+}/Co to be close to each other. When 3.5 g of NaOH was used in sample S5, the atomic percentages of Fe and Co were also comparable.

Figure 3 shows the SEM and TEM images of the S1, S3, S4, and S5 samples in which the amounts of PVP and NaOH are varied to compare with sample S2. When 2.5 g of NaOH was used without PVP (sample S1), the large particles with a lot of small irregular nanoplates were obtained (Fig. 3(a) and 3(b)). Shape of the large particles could not be clearly identified; it is likely composed of the self-assembly of polyhedral particles. When PVP was increased to 4 g (sample S3), the large polyhedral with

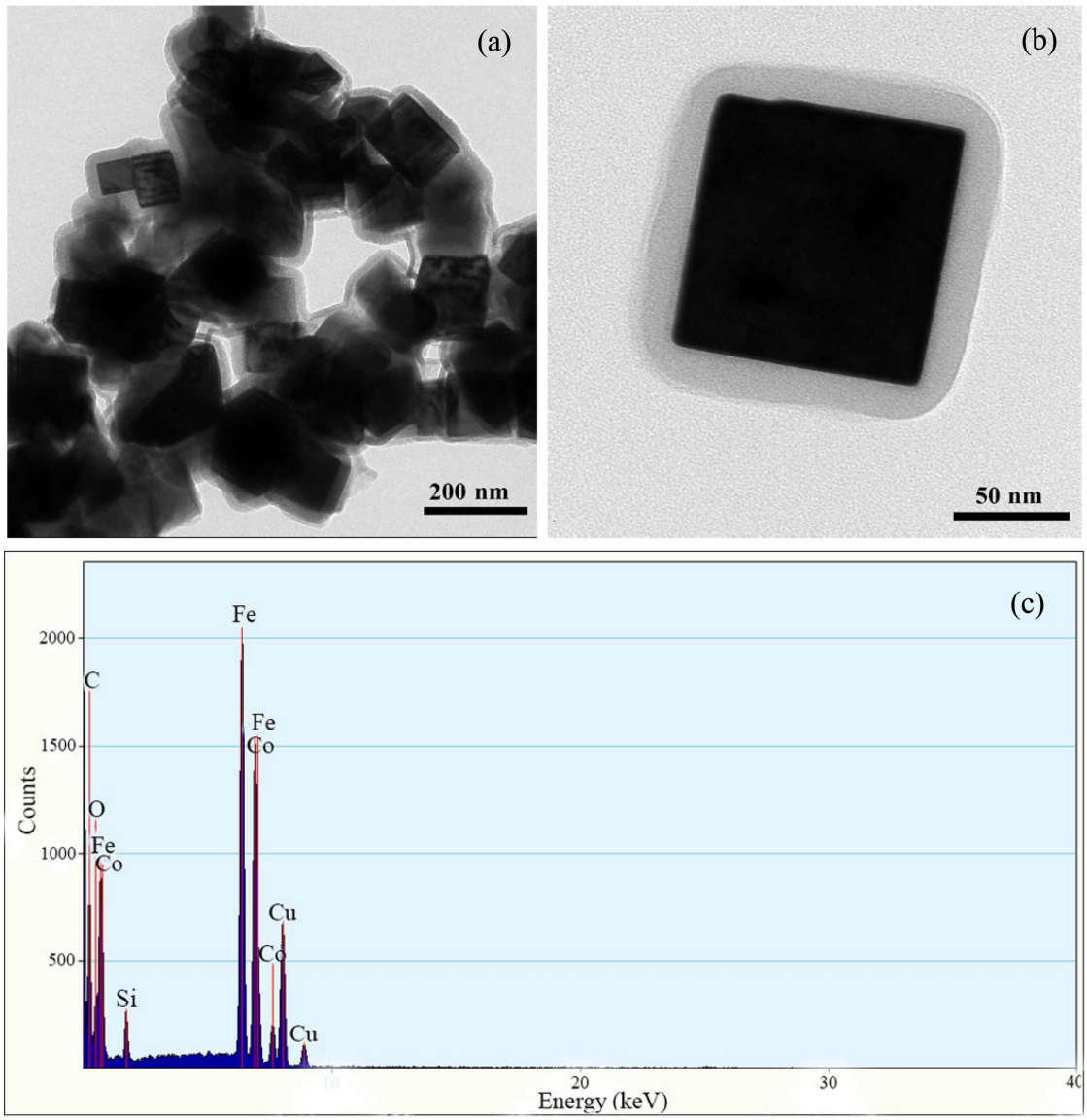

Fig. 4. (Color online) TEM images of the silica coated FeCo nanocubes (a) agglomerated particles, and (b) the isolated particle. Spectrum in (c) is the EDS result determined form the agglomerated silica coated FeCo nanocubes.

some small cubic particles were obtained (Fig. 3(c) and 3(d)). This consequence is similar to the previous report [23] in which 4.0 g of PEG-8000 was used in the synthesis.

PVP has been also employed as a stabilizing polymer in the shape-controlled synthesis of silver nanocubes [29]. It is suggested that PVP could be adsorbed on the {100} planes, and hence reduces the growth rate along <100> direction. The regular cubic particles could be generated when the ratio between the growth rates along <100> and <111> directions approach to 0.58 [30]. Regarding this mechanism, the different amounts of PVP could alter the growth rates leading to the variation in particle morphology. However, it should be noted that the bonding geometry and the selectivity of PVP adsorption between different crystallographic planes are still not clear. In the previous report [22], when PEG was used as a capping agent, cyclohexane is proposed to play an essential role in the adsorption of the PEG on the crystallographic planes. This contrast reveals that the polymer-adsorption mechanism likely depends on nature of the polymer used. The concentration of NaOH also affects the particle morphology. When the optimized amount of PVP (2.0 g) was used, and the concentration of NaOH was decreased to 0.75 M (sample S4), the sample was composed of irregular shape particles with some nanocubes and nanorods (Fig. 3(e) and 3(f)). However, when the concentration of NaOH was increased to 1.75 M (sample S5), the particles with a well-defined cubic shape were also obtained (Fig. 3(g)

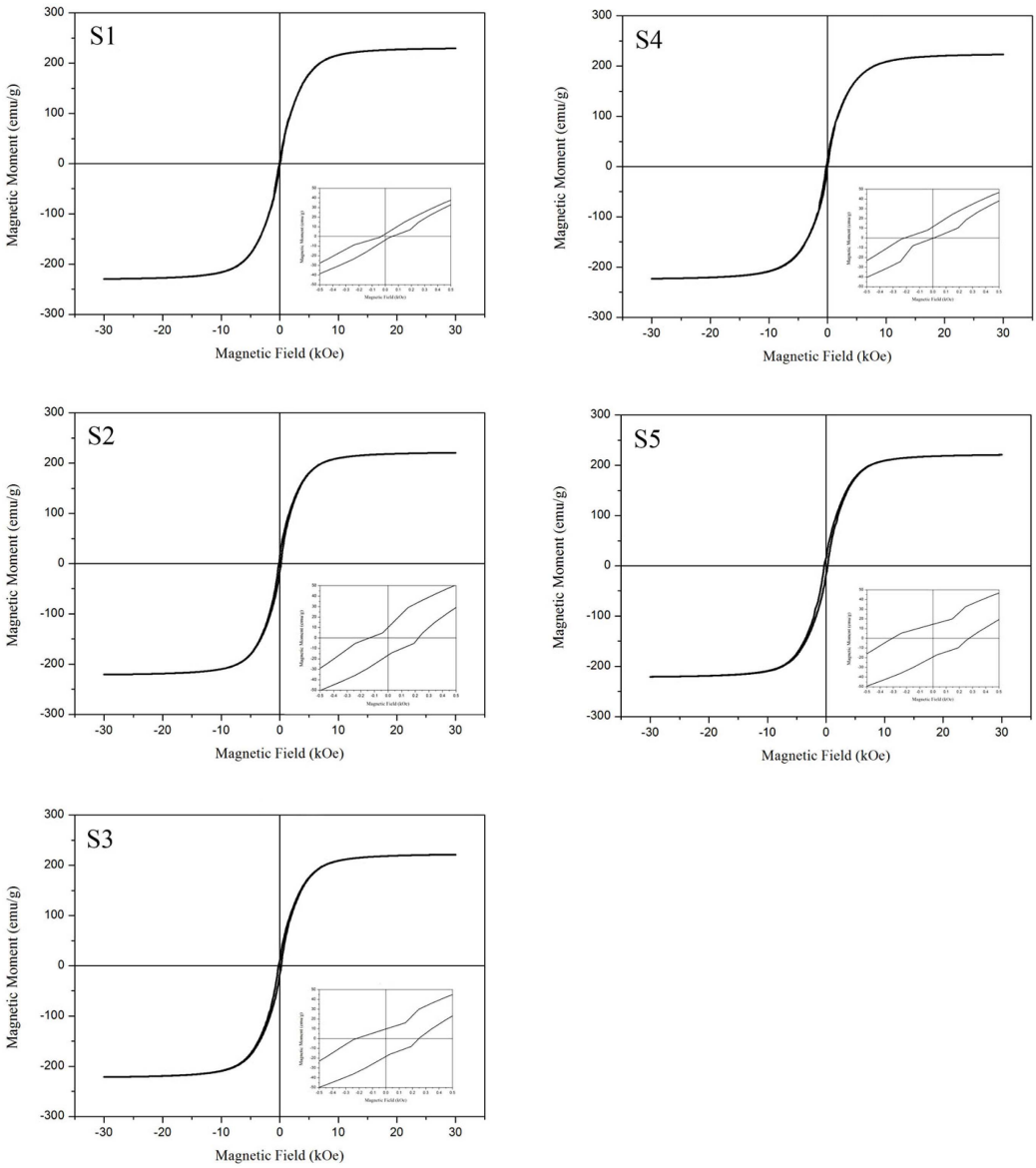

Fig. 5. Magnetic hysteresis loops of the samples. Insets show the extended view at low magnetic field.

and 3(h)). These results indicate that the concentration of NaOH at least 1.25 M needs to be used to obtain the well-defined shape FeCo nanocubes. In addition, when no any capping polymer was used, 0.5 M of NaOH resulted in the large FeCo nanocubes with small irregular-shape $CoFe_2O_4$. By increasing the concentration of NaOH to eliminate the $CoFe_2O_4$ nanoparticles, the flower-like structured FeCo particles were obtained instead of the cubic [27]. The effect of NaOH concentration on the particle morphology might relate to the amounts of Fe^{2+} and Co^{2+} at the early state of the particle formation. As reported in the previous works [27], the amounts of Fe^{2+} and Co^{2+} are proportional to the concentration of NaOH, and the FeCo flower-like structures are also obtained when the molar ratio of Fe^{2+} and Co^{2+} is 1:3 [22]. These results indicate that the amounts of PVP and NaOH have to be optimized to obtain single-phase FeCo nanocubes. PVP controls the growth rates at specific directions, and NaOH results in the Fe/Co ratio at the early state of the particle formation which also affects the particle morphology [26].

3.3. Silica coating

Figure 4. illustrates the TEM images and EDS spectrum of silica coated FeCo nanocubes. The isolated FeCo nanocube could be coated with the silica with a shell thickness of around 17 nm (Fig. 4(b)). The EDS spectrum shown in Fig. 4(c) indicates the presence of Si and O peaks which confirm that the nanocubes are coated with the silica. Additionally, the atomic percentage of oxygen is higher than that of Si more than 2 times implying the presence of SiO_2. Nevertheless, it should be realized that because the particles tend to agglomerate, the silica could be deposited on some aggregated particles (Fig. 4(a)). To prevent the particle agglomeration, they have to be further coated with another capping agent that can increase the steric and/or electric repulsive forces, to counterbalance with the van der Waals attractive forces [31].

3.4. Magnetic Properties

Hysteresis loops of the as-prepared FeCo particles are shown in Fig. 5. The saturation magnetization (M_s) of S1, S2, S3, S4, and S5 are as high as 229.6, 220.9, 221.6, 223.3, and 220.9 emu/g, respectively. These values are well comparable to the M_s of bulk $Fe_{50}Co_{50}$ alloy (220 emu/g) [32], indicating that the compositions of as-prepared FeCo particles are close to 50:50, and oxide layer is not present on the particle surface [33]. Abbas *et al.* [11] reported that the saturation magnetization increases with the Fe proportion and reaches the maximum at $Fe_{60}Co_{40}$. All samples also exhibited the low remanent magnetization (M_r) and coercivity (H_c), for example, the M_r and H_c of sample S2 in which mostly consisted of FeCo nanocubes were of 4.8 emu/g and 180 Oe, respectively. These values are nearly superparamagnetic, and would be useful in some biomedical applications. Insets shown in Fig. 5 illustrate the difference in coercivities of the samples which are in between 60 and 220 Oe. Coercivity of FeCo particles is dependent on various factors including shape anisotropy and composition of the particles. Rod shaped FeCo particles display high coercivity around 1158 Oe [34] whereas spherical FeCo particles possess low coercivity below 100 Oe [17]. Higher coercivity can be obtained in high Co content particles due to the higher anisotropy energy of Co compared to that of Fe [35]. Therefore, fluctuation of coercivity in the present work can be ascribed to the variation of particle shape and composition.

4. Conclusions

The air-stable FeCo nanocubes have successfully synthesized by the facile chemical reduction. The concentrations of PVP and NaOH were found as the key factors in control of the particle morphology. The non-optimized concentration of PVP promoted the large polyhedral-shape particles while the insufficient concentration of NaOH generated the irregular-shape particles with some nanorods. In addition, because PVP was used as the capping polymer, silica could be directly deposited on the surfaces of FeCo nanocubes. The as-prepared FeCo nanocubes also showed the very high M_s and low H_c. However, the prevention of particle agglomeration and self-organization of the FeCo nanocubes would be challenging tasks.

Acknowledgments

This work is financial supported by Synchrotron Light Research Institute (Public Organization) and the Thailand Research Fund (TRF) under Grant No. TRG5980002. The authors also acknowledge the Department of Physics, Khon Kaen University for VSM and TEM measurements.

References

[1] A. R. Tao, S. Habas, and P. Yang, Small **4**, 310 (2008).
[2] B. Wiley, Y.-G. Sun, and Y.-N. Xia, Acc. Chem. Res. **40**, 1067 (2007).
[3] Y.-N. Xia and N. J. Halas, MRS Bull. **30**, 338 (2005).
[4] Q. Song and Z. J. Zhang, J. Am. Chem. Soc. **126**, 6164 (2004).
[5] T. Sau and A. L. Rogach, Adv. Mater. **22**, 1781 (2010).
[6] M. Chen, J.-M. Kim, H.-Y. Fan, and S.-H. Sun, J. Am.

Chem. Soc. **128**, 7132 (2006).
[7] G.-H. Gao, X.-H. Liu, R.-R. Shi, K.-C. Zhou, Y.-G. Shi, R.-Z. Ma, E. Takayama-Muromachi, and G.-Z. Qiu, Cryst. Growth Des. **10**, 2888 (2010).
[8] S-II. Choi, S.-U. Lee, W. Y. Kim, R. Choi, K. Hong, K. M. Nam, S. W. Han, and J. T. Park, ACS Appl. Mater. Inter. **4**, 6228 (2012).
[9] K. Zhang, O. Amponsah, M. Arslan, T. Holloway, W. Cao, and A. K. Pradhan, J. Appl. Phys. **111**, 07B525 (2012).
[10] X. Fan, H. Gao, X. Kou, B. Zhang, and S. Wang, Mater. Res. Bull. **65**, 320 (2015).
[11] M. Abbas, N. Islam, B. P. Rao, T. Ogawa, M. Takahashi, and C. Kim, Mater. Lett. **91**, 326 (2013).
[12] I. Robinson, S. Zacchini, L. D. Tung, S. Maenosono, and N. T. K. Thanh, Chem. Mater. **21**, 3021 (2009).
[13] T. L. Kline, Y.-H. Xu, Y. Jing, and J.-P. Wang, J. Magn. Magn. Mater. **321**, 1525 (2009).
[14] I. Koh and L. Josephson, Sensors **9**, 8130 (2009).
[15] J.-N. Kim, J.-B. Kim, J.-R. Kim, and H. Kim, J. Appl. Phys. **113**, 17A313 (2013).
[16] G. S. Chaubey, C. Barcena, N. Poudyal, C.-B. Rong, J.-M. Gao, S.-H. Sun, and J. P. Liu, J. Am. Chem. Soc. **129**, 7214 (2007).
[17] V. Tzitzios, G. Basina, D. Niarchaos, W. Li, and G. Hadjipanayis, J. Appl. Phys. **109**, 07A313 (2011).
[18] Z. J. Huba, K. J. Carroll, and E. E. Carpenter, J. Appl. Phys. **109**, 07B514 (2011).
[19] S. J. Lee, J.-H. Cho, C. Lee, J. Cho, Y.-R. Kim, and J. K. Park, Nanotechnology **22**, 375603 (2011).
[20] C. W. Kim, Y. H. Kim, H. G. Cha, H. W. Kwon, and Y. S. Kang, J. Phys. Chem. B. **110**, 24418 (2006).
[21] D. Kodama, K. Shinoda, K. Sata, Y. Konno, R. J. Joseyphus, K. Motomiya, H. Takahashi, T. Matsumoto, Y. Sato, K. Tohji, and B. Jeyadevan, Adv. Mater. **18**, 3154 (2006).
[22] X.-W. Wei, G.-X. Zhu, Y.-J. Liu, Y.-H. Ni, Y. Song, and Z. Xu, Chem. Mater. **20**, 6248 (2008).
[23] K. Chokprasombat, P. Harding, S. Pinitsoontorn, and S. Maensiri, J. Magn. Magn. Mater. **369**, 228 (2014).
[24] A. G. Kolhatkar, I. Nekrashevich, D. Litvinov, R. C. Willson, and T. R. Lee, Chem. Mater. **25**, 1092 (2013).
[25] A.-H. Lu, E. L. Salabas, and F. Schüth, Angew. Chem. Int. Ed. **46**, 1222 (2007).
[26] S. J. Yan, L. Zhen, C. Y. Xu, J. T. Jiang, W. Z. Shao, and J. K. Tang, J. Magn. Magn. Mater. **323**, 515 (2011).
[27] M. Y. Rafique, L. Pan, M. Z. Iqbal, Qurat-ul-ain. Javed, H. Qiu, Rafi-ud-din, M. H. Farooq, and Z. Guo, J. Alloy. Compd. **550**, 423 (2013).
[28] W. H. Qi and M. P. Wang, J. Nanopart. Res. **7**, 51 (2005).
[29] Y. Sun and Y.-N. Xia, Science **298**, 2176 (2002).
[30] Z. L. Wang, J. Phys. Chem. B **104**, 1153 (2000).
[31] A. R. Studart, E. Amstad, and L. J. Gauckler, Langmuir **23**, 1081 (2007).
[32] C. Kuhrt and L. Schultz, J. Appl. Phys. **73**, 6588 (1993).
[33] P. Karipoth, A. Thirumurugan, and R. J. Josephus, J. Colloid. Interf. Sci. **404**, 49 (2013).
[34] M. Farahmandjou, S. Honarbakhsh, and S. Behrouzinia, J. Supercond. Nov. Magn. **31**, 4147 (2018).
[35] K. P. Santosh and D. Bahadur, Mater. Lett. **64**, 1127 (2010).